Eur J Vasc Endovasc Surg 26, 367–373 (2003)
doi: 10.1016/S1078-5884(03)00243-0, available online at http://www.sciencedirect.com on SCIENCE DIRECT

Local Haemodynamics and Shear Stress in Cuffed and Straight PTFE-venous Anastomoses: an in-vitro Comparison using Particle Image Velocimetry

M. Heise,*[1] S. Schmidt,[1] U. Krüger,[2] R. Pfitzmann,[1] H. Scholz,[2] P. Neuhaus[1] and U. Settmacher[1]

Departments of [1]General Surgery, Humboldt University, Charité, Campus Virchow Klinikum, and [2]Vascular Surgery, Königin Elisabeth Krankenhaus, Berlin, Germany

Objectives: *To use particle image velocimetry (PIV) to study the haemodynamics and shear stress associated with cuffed and straight PTFE-venous anastomoses.*
Methods: *Silastic models of a straight and cuffed (Venaflo™) PTFE-venous anastomoses were attached to a pulsatile flow 'Berlin Heart' circuit filled with glycerine/water and hollow glass tracer spheres. Instantaneous velocity fields were obtained PIV and shear rates and patterns calculated from frame-by-frame analysis.*
Results: *A high velocity jet struck the anastomotic 'floor' and was deflected toward the venous outflow. Shear stresses near the floor were significantly higher, in the straight anastomosis. Sites of high shear stress correlated well with the known sites of intimal hyperplasia.*
Conclusions: *A cuffed anastomosis type may be favourable in terms of local haemodynamics so enhancing the long-term patency of PTFE-venous grafts.*

Key Words: Hemodialysis; Vascular access; Intimal hyperplasia; Anastomosis geometry; Particle image velocimetry.

Introduction

Autologous arteriovenous fistula (AVF) are clearly preferable to PTFE grafts for long-term haemodialysis in terms of patency and infection rates, and costs.[1–5] The commonest cause of PTFE graft failure is intimal hyperplasia (IH) at the venous anastomoses.[6,7] Unlike arterial hyperplasia, which appears to represent an adaptation of the vessel wall to low-shear stress, little is known about venous hyperplasia.[8–10] Several in-vitro studies have used flow visualization techniques or computational fluid dynamics algorithms in order to define the local haemodynamics inside cuffed and straight configured arteriovenous PTFE grafts.[11–15] Particle image velocimetry (PIV) combines both flow visualization and high resolution velocity measurements.[16,17] The velocity maps obtained using PIV also allow computation of other important parameters such as shear rates, stresses and vorticity.[16,18] We therefore investigated the local haemodynamics of cuffed and straight configured arteriovenous grafts in an artificial circulation by means of PIV. The aim of this study was to use PIV to study the haemodynamics and shear stress associated with cuffed and straight PTFE-venous anastomoses.

*Corresponding author. Michael Heise, Department of General Surgery, Humboldt University, Augustenburger Platz 1, Charité, Campus Virchow Klinikum, Berlin 13353, Germany.

Material and Methods

Silastic models of a straight and cuffed (Venaflo™) PTFE-venous anastomoses were fabricated (Fig. 1). The diameter of the recipient vein was 6 mm and the graft diameter was 7 mm. The maximum diameter of the cuffed anastomosis central region was 15 and 10 mm for the straight form, respectively. Anastomoses were attached to a pulsatile flow 'Berlin Heart' circuit (1 cm tubes). The flow rate was measured by an ultrasound flow meter (T206, Transonic Systems, Ithaca, USA) and the pressure was measured by a Statham transducer element (Transpac IV, Abbott Laboratories, Morgan Hill, USA). The distal antegrade and retrograde outlets were connected to the venous reservoir, which provided a venous pressure of 15 mmHg. The PIV measurements were taken at mean flow rates of 500 ml/min. A solution containing

1078–5884/03/000367 + 07 $35.00/0 © 2003 Elsevier Ltd. All rights reserved.

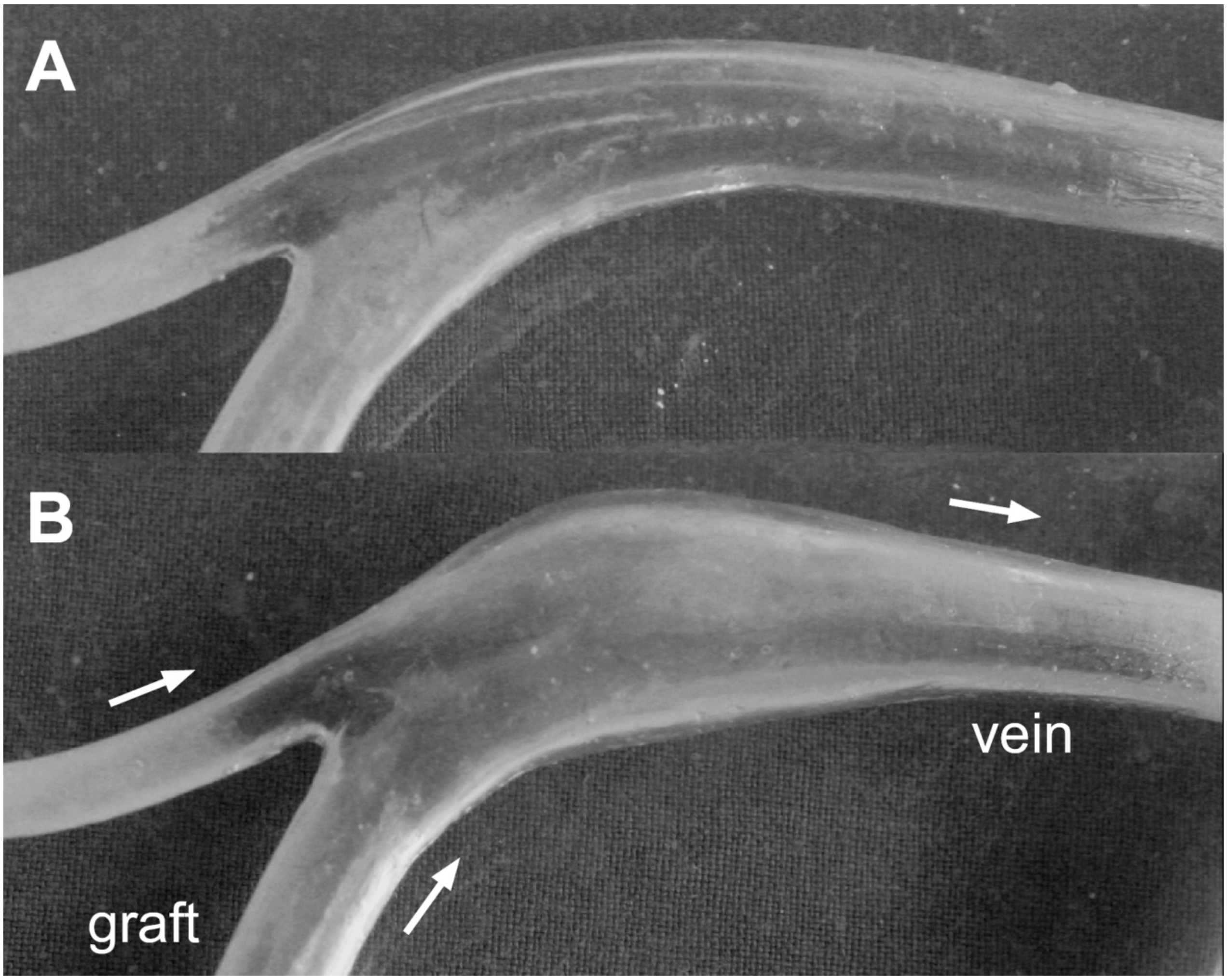

Fig. 1. Photograph showing the silastic models used for measurement of local hemodynamics. A = straight arteriovenous graft, B = cuffed graft type (Venaflo™). Arrows depicting flow direction.

about 42% glycerine (Merck, Darmstadt, Germany) and 58% water was used to provide a fluid with a viscosity comparable to blood. The resulting viscosity was measured by means of a capillary viscosimeter (Cavis, Raczek, Wedemark, Germany) and the mixture adapted to yield a viscosity of 4 mPa s. Hollow glass spheres with a mean size of 9–13 μm (Sphericel, Potters Industries, Parsippany, USA) were used as tracer particles and seeded into the fluid. A circulating heating pump was inserted into the fluid reservoir to ensure uniform distribution of the glass spheres at a temperature of 25°C.

Particle Image Velocimetry

The PIV technique allows the instantaneous acquisition of an entire flow field. The light of a double pulsed Nd:Yag laser (Minilite, Continuum, Santa Clara, USA) was directed through a cylindrical lens

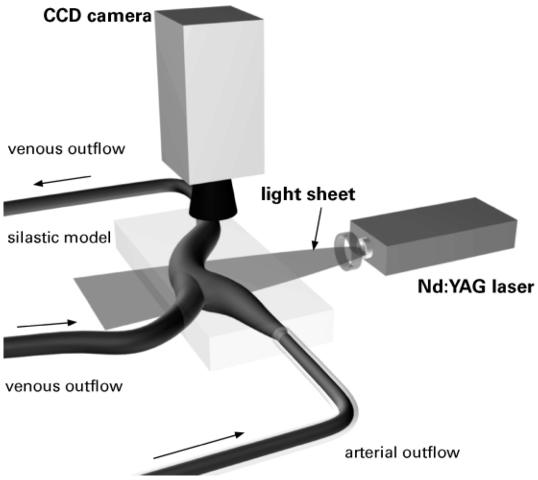

Fig. 2. Diagram showing the Particle image velocimetry setting. A laser light sheet is used to illuminate a central plane of the fluid.

where it diverged and formed a light sheet (Fig. 2). The sheet was used to illuminate a central plane of the fluid flow. The motion of the seeded particles was recorded twice, using a delay of 500 μs, by means of a CCD-Camera (Flowmaster II, Lavison, Göttingen, Germany), which was positioned at 90° to the laser sheet. The displacement of the particles between the two-recorded images was directly proportional to the local fluid velocity. The images were analyzed using a cross-correlation algorithm yielding the local displacement vector for each interrogation area (Davis 6.2, Lavision, Göttingen, Germany). The laser timing unit was triggered to the beginning of the systole by means of the flowmeter signal. This allowed a frame-by-frame analysis of selected time points within the cardiac cycle. PIV measurements were obtained sequentially at recurring 100 ms segments beginning 50 ms after the onset of systole. Therefore, using a heart rate of 60/min a total of ten PIV recordings per cardiac cycle were obtained. For each time step five measurements were averaged. Applying a systolic duration of 45%, systole ended after 450 ms. The venous anastomoses and outflow areas were mapped using sequential measurements taken at different parts of the anastomoses. The individual recordings were eventually used to reconstruct the entire anastomosis (Fig. 3).

Postprocessing of the Data

The vector data for each interrogation area were visualized using an arrow with a length proportional to the local fluid velocity (Fig. 3). For comparison of mean velocities at comparable regions within the anastomoses, rectangular areas covering 20–30 vectors were selected and averaged for each time step.

The velocity fields obtained by PIV were furthermore used to calculate shear rates shear stress and vorticity (fluid rotation in z-direction) using the partial derivatives of the velocity components to both x and y (Figs 3 and 4).[18] The shear stresses near the venous floor were calculated for four areas (Fig. 3).

Statistics

Data are expressed as mean ± standard deviation. A Student t test was used to compare velocities and shear stresses at the venous floor. P-values <0.05 were considered statistically significant.

Results

The flow visualization revealed a high velocity jet entering the anastomoses center of both forms, striking on the venous floor and turning toward the distal outflow (Fig. 3). During the acceleration phase of the systole a small retrograde venous flow was visible toward the incoming vein. At the hood region of both the straight and the cuffed anastomoses a large separation area developed, which lasted through the entire cardiac cycle. The mainstream of the straight form showed a sharp deflection near the venous wall toward the distal venous outlet, while the velocity distribution within the Venaflo™ was more homogenous, which was attributed to the larger anastomosis area. The highest shear stresses were found near the venous wall where the mainstream jet impinged on the venous floor. Along the upstream wall of the recipient vein the shear stresses were finally decreasing in both anastomoses.

However, the systolic shear stresses inside the straight form were significantly higher compared to the cuffed anastomosis, while the velocities near the venous floor were comparable for both anastomotic configurations (Fig. 5). Mean systolic centerline velocities at the deflection point of the conventional form were 0.29 ± 0.09 m/s and 0.31 ± 0.08 m/s at comparable areas of the Venaflo™ (measured at 500 ml/min) ($p =$ n.s.).

The vorticity (flow rotation in z-direction) distribution was more uniform inside the cuffed anastomosis showing smooth transitions between mainstream and separations zones (Fig. 4). In contrast, the vorticity pattern, particularly at the high shear stress areas near the venous floor, was very irregular presenting with higher peak vorticities and wider high vorticity regions compared to the Venaflo™ anastomosis. A significant reduction of vorticity strength was observed for several locations inside the cuffed anastomosis compared to the straight graft. Especially at the turning point of the high velocity mainstream towards the venous inlet and along the transition zone between the mainstream and the large hood separation the total flow circulation was decreased.

Discussion

Unfortunately, about 60% of synthetic grafts fail within the first year after surgery mainly due to the development of IH at the venous anastomosis.[19–21] However unlike arterial remodeling, which develops in areas with low shear stresses, the onset of venous IH is probably due to high shear flow.[9,10,22,23] Similar to

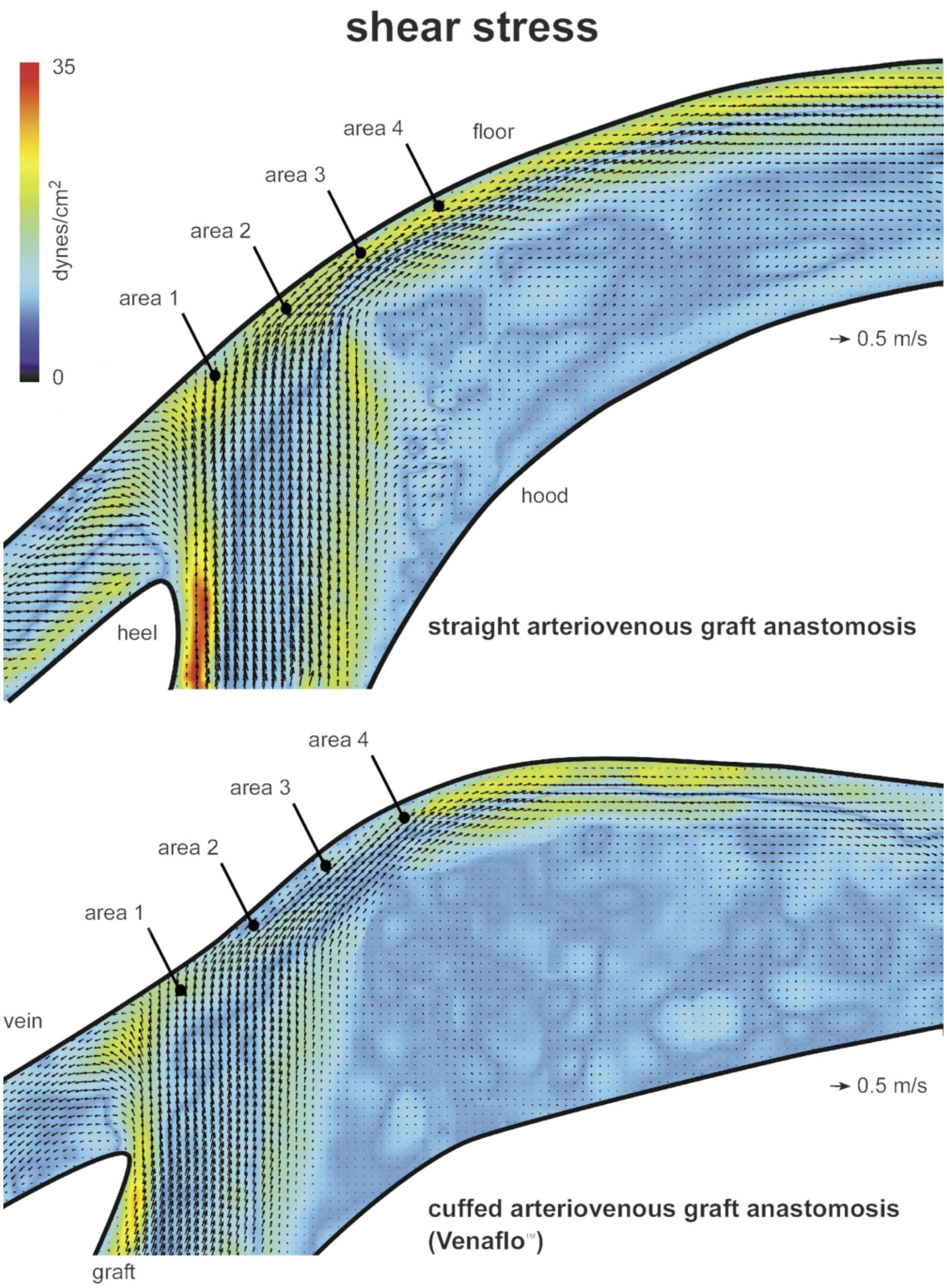

Fig. 3. Reconstruction of the velocity fields obtained using particle image velocimetry. A high velocity mainstream entered the central anastomosis turning toward the venous outflow. Large separation areas developed at the toe of the anastomoses. Comparison of four selected areas near the venous floor revealed significantly higher shear stresses inside the straight graft, even though velocities were comparable.

arterial hyperplasia is the venous type of IH equally limited to certain points within the venous anastomoses. A number of animal studies using PTFE loops reported a uniform distribution of IH inside the venous anastomoses.[9,13,24] In all studies, the site of maximum IH was found on the floor of the recipient vein opposite of the anastomotic hood. The local development was attributed to local flow disturbances although the exact flow environment in this area has not been defined. However, several flow visualization and computational fluid dynamics studies showed that a high velocity jet entered the anastomosis impinging on the venous floor and it appeared that the point of maximum velocity impingement correlated with the site of maximum IH development.[13,25–27] The use of PIV provided both flow visualization

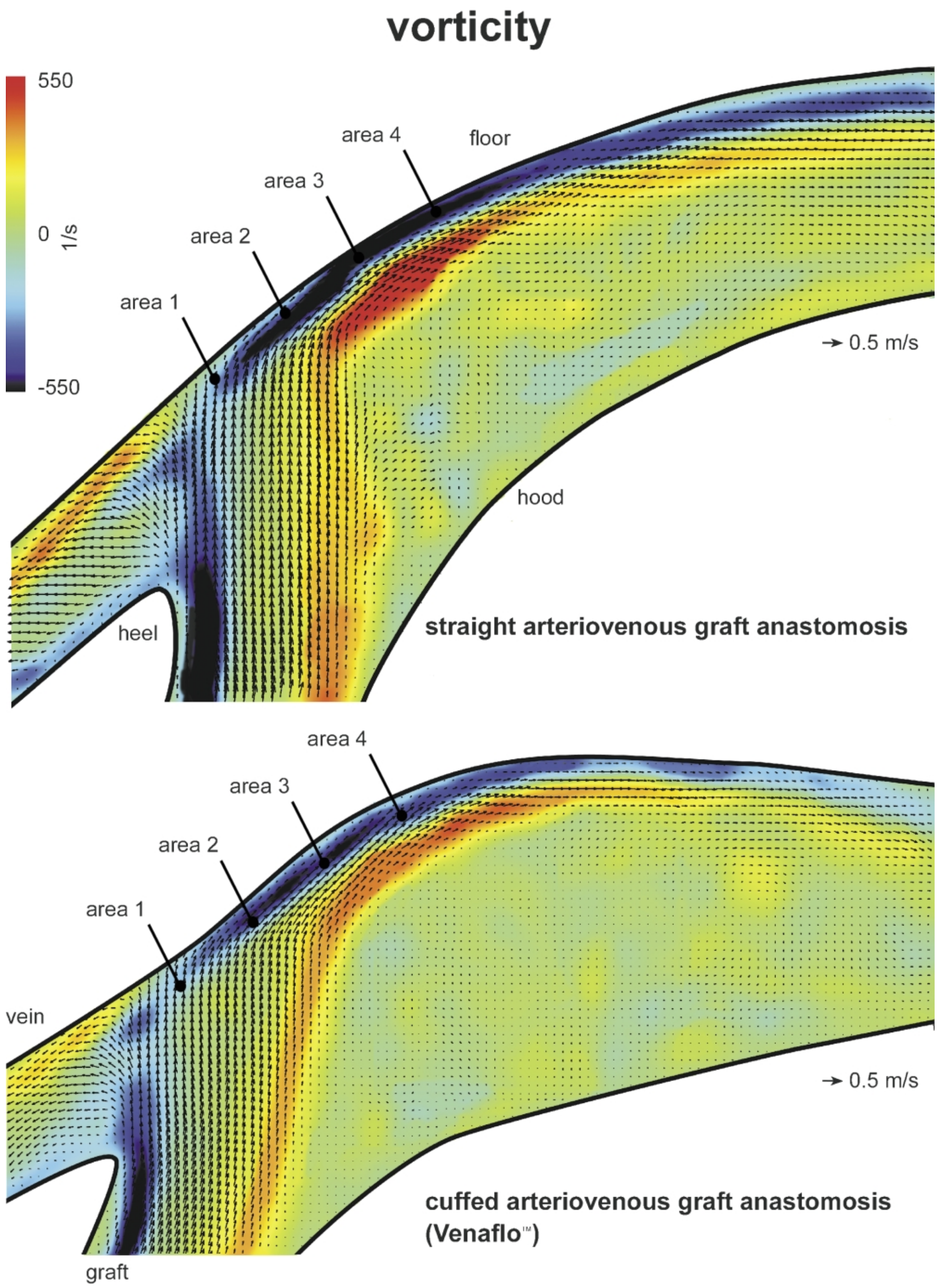

Fig. 4. Velocity and vorticity (rotation in *z*-direction) plots of the straight and cuffed (Venaflo™) arteriovenous PTFE graft anastomoses. The vorticity pattern inside the cuffed form was more homogenously distributed. The transition zones between mainstream and separation of the straight anastomosis were wider and the vorticity peak levels were higher compared to the cuffed design.

and high resolution velocity measurements. The velocity fields obtained with this method allowed computation of shear rates and shear stresses as well as vorticity in a high resolution. Vorticity is a measure of local fluid rotation in *z*-direction indicating rotational shear forces. The flow visualization revealed the non-uniform distribution of the high velocity mainstream with higher velocities on the lateral than on the medial wall of the graft. The mainstream entered the anastomosis center forming a jet with high velocity and momentum, which finally impinged on the floor of the vein. This flow pattern was earlier described by several authors.[14,15,26,27] The mean velocities in the anastomotic center near the venous

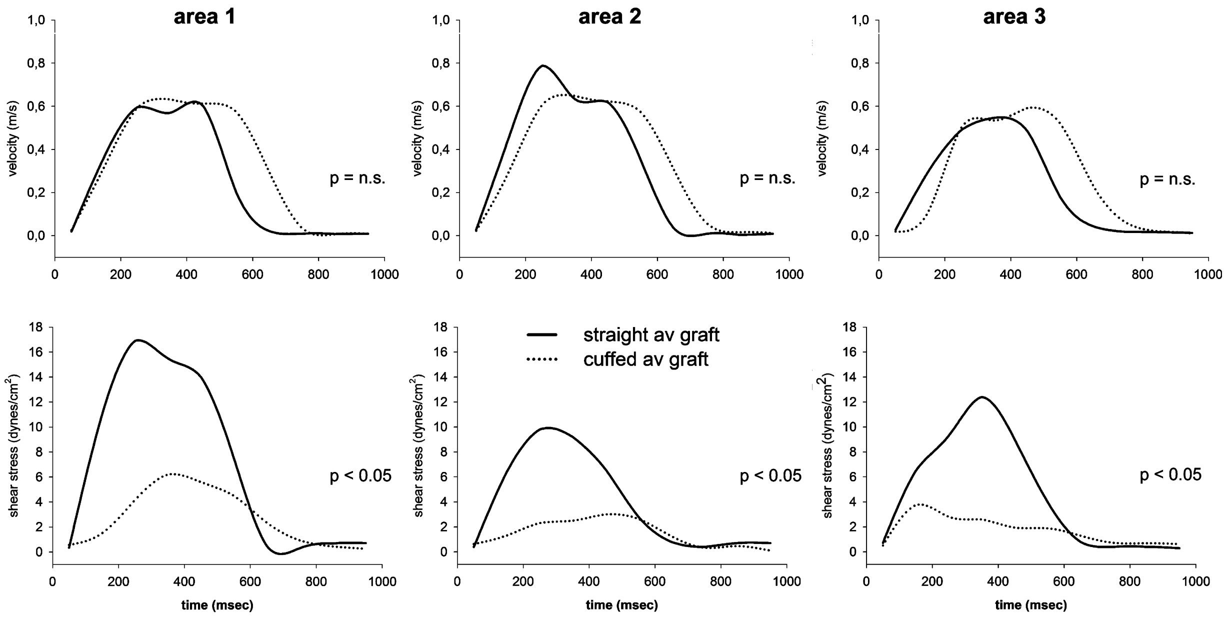

Fig. 5. Comparison of velocity and shear stress profiles at different locations near the venous floor. While the velocity profiles during the cardiac cycle were almost identical, the systolic shear stresses of the straight configured arteriovenous graft were significantly higher.

floor were comparable between the cuffed and the straight form, but there were remarkable differences between the shear forces at these sites. The shear stresses near the venous floor in the straight configuration were much higher compared to the Venaflo™ anastomosis. Although the shear stresses decreased downstream on the floor they were always significantly higher in the straight graft anastomosis. These high shear stress areas were located in the particular area where the mainstream jet impinged on the venous wall and they correlated spatially with the reported regions of maximum IH development. Therefore, in contrast to arterial remodeling as a response to low-shear forces the venous type probably results from high-shear flow creating strong hydraulic forces on the endothelial cells, as previously hypothized by Fillinger, Longest and others.[8–10,26,27]

Unfortunately, unlike the proliferative response of the arterial wall to low-shear, little is known about the biological sequence of venous hyperplasia. The arterial remodeling represents an adaptation of the wall in order to re-establish normal shear stress levels (5–30 dynes/cm^2). It was shown that endothelial cells are capable of sensing shear stress and are able to modulate biological processes that lead to proliferation of subendothelial cells resulting in the wall thickening known as IH.[28–30] The purpose of the hyperplastic response of the vein wall and the underlying biologic pathways remain unknown. The abrupt increase in pressure, distension, vessel diameter and wall shear stress, probably leads to the hyperplastic response to reinforce the vein wall, in order to stabilize it and prevent a rupture, but this remains speculative. However, the site of maximum hyperplasia development coincides with the point where maximum mechanical forces are acting on the venous wall.

In this regard, one aspect is particularly important. The wider anastomosis area of the cuffed anastomosis obviously mitigates the peak shear stresses by providing a wider mainstream with a more homogenous velocity and vorticity distribution. This is supported by the fact, that both the shear stresses near the venous floor as well as the flow rotation (indicated by vorticity strength) within the anastomosis center were significantly decreased in the cuffed anastomosis. The assumed benefits of the cuffed anastomosis type were confirmed by recent randomized clinical trials using the new cuffed Venaflo™ graft for haemodialysis access.[31,32] They clearly demonstrated the superiority of the Venaflo™ graft in terms of patency compared with a conventional straight PTFE graft. In addition, a venous outflow stenosis was three times more frequently observed in the standard group than in the Venaflo™ group.

In summary, the results of this study support the use of the cuffed PTFE graft for haemodialysis access. The wall shear stresses near the venous floor were significantly lower in the Venaflo™ anastomosis, hypothetically preventing the hyperplastic response of the vessel wall.

Acknowledgements

This study was supported in part by the Else Kröner-Fresenius-Stiftung, Bad Homburg, Germany. The authors would like to thank Ronald Aeberhard, Seattle, USA, for his editorial assistance.

References

1 Patel NH, Revanur VK, Khanna A, Hodges C, Jindal RM. Vascular access for hemodialysis: an indepth review. *J Nephrol* 2001; **14**(3): 146–156.

2 Besarab A. Preventing vascular access dysfunction: which policy to follow. *Blood Purif* 2002; **20**(1): 26–35.

3 Feldman HI, Held PJ, Hutchinson JT, Stoiber E, Hartigan MF, Berlin JA. Hemodialysis vascular access morbidity in the United States. *Kidney Int* 1993; **43**(5): 1091–1096.

4 Nassar GM, Ayus JC. Infectious complications of the hemodialysis access. *Kidney Int* 2001; **60**(1): 1–13.

5 Hakim R, Himmelfarb J. Hemodialysis access failure: a call to action. *Kidney Int* 1998; **54**(4): 1029–1040.

6 Woods JD, Turenne MN, Strawderman RL, Young EW, Hirth RA, Port FK *et al.* Vascular access survival among incident hemodialysis patients in the United States. *Am J Kidney Dis* 1997; **30**(1): 50–57.

7 Hofstra L, Bergmans DC, Leunissen KM, Hoeks AP, Kitslaar PJ, Tordoir JH. Prosthetic arteriovenous fistulas and venous anastomotic stenosis: influence of a high flow velocity on the development of intimal hyperplasia. *Blood Purif* 1996; **14**(5): 345–349.

8 Fillinger MF, Reinitz ER, Schwartz RA, Resetarits DE, Paskanik AM, Bredenberg CE. Beneficial effects of banding on venous intimal-medial hyperplasia in arteriovenous loop grafts. *Am J Surg* 1998; **158**(2): 87–94.

9 Fillinger MF, Reinitz ER, Schwartz RA, Resetarits DE, Paskanik AM, Bruch D *et al.* Graft geometry and venous intimal-medial hyperplasia in arteriovenous loop grafts. *J Vasc Surg* 1990; **11**(4): 556–566.

10 Hofstra L, Bergmans DC, Leunissen KM, Hoeks AP, Kitslaar PJ, Daemen MJ *et al.* Anastomotic intimal hyperplasia in prosthetic arteriovenous fistulas for hemodialysis is associated with initial high flow velocity and not with mismatch in elastic properties. *J Am Soc Nephrol* 1995; **6**(6): 1625–1633.

11 Shu MC, Hwang NH. Flow phenomena in compliant and noncompliant arteriovenous grafts. *ASAIO Trans* 1988; **34**(3): 519–523.

12 Shu MC, Noon GP, Hwang NH. Phasic flow patterns at a hemodialysis venous anastomosis. *Biorheology* 1987; **24**(6): 711–722.

13 Shu MC, Hwang NH. Haemodynamics of angioaccess venous anastomoses. *J Biomed Eng* 1991; **13**(2): 103–112.

14 Krueger U, Zanow J, Scholz H. Computational fluid dynamics and vascular access. *Artif Organs* 2002; **26**(7): 571–575.

15 Krueger U, Zanow J, Scholz H. Comparison of two different arteriovenous anastomotic forms by numerical 3D simulation of blood flow. *Int J Angiol* 2000; **9**: 226–231.

16 Raffel M, Willert C, Kompenhans J. *Particle Image Velocimetry.* Berlin/Heidelberg/New York: Springer-Verlag, 1998.

17 Westerweel J. Fundamentals of digital particle image velocimetry. *Meas Sci Technol* 1997; **8**: 1379–1392.

18 Stamhuis E, Videler J. Quantitative flow analysis around aquatic animals using laser sheet particle image velocimetry. *J Exp Biol* 1995; **198**: 283–294.

19 Munda R, First MR, Alexander JW, Linnemann Jr. CC, Fidler JP, Kittur D. Polytetrafluoroethylene graft survival in hemodialysis. *JAMA* 1983; **249**(2): 219–222.

20 Tordoir JH, Herman JM, Kwan TS, Diderich PM. Long-term follow-up of the polytetrafluoroethylene (PTFE) prosthesis as an arteriovenous fistula for haemodialysis. *Eur J Vasc Surg* 1988; **2**(1): 3–7.

21 Culp K, Flanigan M, Taylor L, Rothstein M. Vascular access thrombosis in new hemodialysis patients. *Am J Kidney Dis* 1995; **26**(2): 341–346.

22 Salam T, Lumsden A, Suggs W, Ku DN. Low shear stress promotes intimal hyperplasia thickening. *J Vasc Invest* 1996; **2**(1): 12–22.

23 Gibbons GH, Dzau VJ. The emerging concept of vascular remodeling. *N Engl J Med* 1994; **330**(20): 1431–1438.

24 Lemson MS, Daemen MJ, Kitslaar PJ, Tordoir JH. A new animal model to study intimal hyperplasia in arteriovenous fistulas. *J Surg Res* 1999; **85**(1): 51–58.

25 Shu MC, Noon GP, Hwang NH. Flow profiles and wall shear stress distribution at a hemodialysis venous anastomosis: preliminary study. *Biorheology* 1987; **24**(6): 723–735.

26 Longest PW, Kleinstreuer C. Computational haemodynamics analysis and comparison study of arterio-venous grafts. *J Med Eng Technol* 2000; **24**(3): 102–110.

27 Longest PW, Kleinstreuer C, Andreotti PJ. Computational analyses and design improvements of graft-to-vein anastomoses. *Crit Rev Biomed Eng* 2000; **28**(1–2): 141–147.

28 Traub O, Berk BC. Laminar shear stress: mechanisms by which endothelial cells transduce an atheroprotective force. *Arterioscler Thromb Vasc Biol* 1998; **18**(5): 677–685.

29 Tai LK, Okuda M, Abe J, Yan C, Berk BC. Fluid shear stress activates proline-rich tyrosine kinase via reactive oxygen species-dependent pathway. *Arterioscler Thromb Vasc Biol* 2002; **22**(11): 1790–1796.

30 Davies PF. Flow-mediated endothelial mechanotransduction. *Physiol Rev* 1995; **75**(3): 519–560.

31 Nyberg SL, Hughes CB, Valenzuela YM, Jenson BM, Benda MM, McCarthy JT *et al.* Preliminary experience with a cuffed ePTFE graft for hemodialysis vascular access. *ASAIO J* 2001; **47**(4): 333–337.

32 Sorom AJ, Hughes CB, McCarthy JT, Jenson BM, Prieto M, Panneton JM *et al.* Prospective, randomized evaluation of a cuffed expanded polytetrafluoroethylene graft for hemodialysis vascular access. *Surgery* 2002; **132**(2): 135–140.

Accepted 14 April 2003